Efficient Techniques for Accelerating the Ray-Tracing for Computing the Multiple Bounce Scattering of Complex Bodies Modeled by Flat Facets

Felipe Cátedra[1], Lorena Lozano[1], Iván González[1], Eliseo García[2], and Mª Jesús Algar[1]

[1] Computer Sciences Department
University of Alcalá, 28871 Alcalá de Henares (MADRID), SPAIN
felipe.catedra@uah.es, lorena.lozano@uah.es, ivan.gonzalez@uah.es, chus.algar@uah.es

[2] Department of Automática
University of Alcalá, 28871 Alcalá de Henares (MADRID), SPAIN
eliseo.garcia@uah.es

***Abstract*—** A new algorithm to accelerate the ray-tracing for computing the radar cross section (RCS) of complex targets is presented. The algorithm is based on a combination of the angular Z-buffer (AZB), the volumetric space partitioning (SVP) and the depth-limited search method. The algorithm is very useful for RCS computing techniques based on geometrical optics (GO) and physical optics (PO). The targets are represented geometrically by a collection of flat patches. The approach is extremely efficient for computations of the RCS of large and complex bodies modeled by a high number of flat surfaces taking into account ray paths with multiple bounces. Results for representative targets are shown.

***Index Terms*—**Radar cross section, physical optics, geometrical optics, ray-tracing.

I. INTRODUCTION

Computer tools for analyzing the RCS of complex objects are very useful for designing platforms with a limited radar echo. In addition, being capable of analyzing the RCS of an object in a particular environment, taking into account the mutual interaction between object and environment, is crucial for the identification of objects on the ground or in the sea. Traditionally, complex targets and their surrounding environments have been modeled with facets; this requires a very large number of facets (tens or hundreds of thousands) for a realistic model. A suitable method for performing the electromagnetic analysis of the reflection of a facet is PO, [1-2] with additional calculations based on equivalent currents method (ECM) [3] to correct the edge effects of the facets. The PO integrals are computed using Gordon's Method for planar surfaces [4] and the stationary phase method (SPM) [5] for curved surfaces. Fresnel´s reflection coefficients are included in the PO approach to take into account radar absorbing materials (RAM) and other materials [6]. Contributions to the RCS from double, triple and higher order reflections between flat facets can be computed assuming that after any reflection the field is collimated in a cylindrical tube and it conserves its plane wave nature in the tube [7-8]. The boundary of the cylindrical tube is defined by projecting the reflection of the silhouette of the facets that have experienced the reflection. In this way, a multiple bounce contribution to the RCS can be computed by a hybrid method that uses GO-GO-….-GO-PO, where GO is used for all reflections except the last, which is evaluated using PO in a similar way. After any bounce the collimated tube is trimmed by the silhouette of the corresponding facet.

Using this approach for RCS analysis with complex targets/environments, most of the CPU-time is spent on determining the facets of the environment that either produce reflection or diffraction— either event will obstruct a ray path. If we consider the problem of finding the RCS of a body modeled by N facets from rays that suffer K bounces, for the incident and observation directions we must identify the sets of K facets that can form ray-paths with K bounces. An exhaustive way to obtain these sets is by forming a search tree [9] (see Fig. 1). In the search tree N branches leave from the node-root (R) to the N

nodes of the first tree level. Each one of the nodes of the first level corresponds to the simple reflection contribution of a facet of the target. (N-1) branches leave from a given node of the first level that correspond with all the double reflection contributions that have the first reflection in that first level node. The third level of the tree has N(N-1)(N-2) nodes, each one of them representing a triple reflection. The subsequent tree levels are formed similarly so that the K^{th} level has N(N-1)(N-2)...(N-K+1) nodes (approximately N^K nodes if N is much greater than K, as usual), where each node of the K^{th} level corresponds to a set of K facets that contribute K reflections. The complexity of the search tree for realistic targets and high order reflection RCS analyses is very high. For instance, a target with 10,000 facets has a tree search with about 10^{16} nodes in the fourth level of the tree— this is unmanageable even for large computers. Of course, not all of the N^K nodes need to be stored or tested for several reasons: the facets of many sets corresponding to the nodes of the K^{th} level are not properly oriented, the ray paths between a pair of facets are obstructed, etc. Thus, as only a very small fraction of the nodes of that level can potentially contribute to the RCS, many tree branches can be pruned at that level or at previous levels. It is numerically very expensive to rigorously check whether or not a facet will suffer a reflection/diffraction. In order to be efficient one should avoid such rigorous checking, discarding facets as early as possible using a fast check.

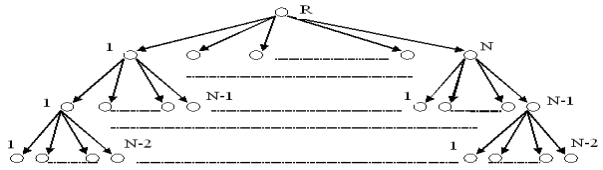

Fig. 1. Search tree for the RCS computation of a given direction considering up to three bounces of a target modeled by N facets.

Recently, in order to speed up the RCS calculation, several ray-tracing acceleration techniques— such as space volumetric partitioning (SVP), binary space partitioning (BSP), angular Z-buffers (AZB), and shooting and bouncing Rays (SBR)—have been developed and applied [10-13]. The underlying philosophy in these algorithms is a fast exploration of the search tree nodes combined with an early pruning of the tree branches: as soon as a node in a given level of the tree search is found to not contribute to the RCS, the node and all its successor nodes are discarded from the RCS analysis. The differences in the performances of the previously mentioned algorithms are due to their different capabilities to quickly explore the tree nodes and pruning the non-contributing tree branches early in the computation. These algorithms have increased the computational capacity: complete RCS processing, including a detailed RCS for images of targets with 50,000 facets and three reflections. The analysis of targets with a larger number of facets and higher orders of reflection is not affordable with the computers available today.

Most of the algorithms mentioned above are based on a non-informed exploration of the search tree, which usually follows a "breadth-first search" strategy [9-14]. In this strategy, to obtain the RCS considering contributions with K bounces, first all the nodes of the first tree level are explored, then all the nodes of the second level and so on until the K^{th} level of the tree is explored (while performing appropriate pruning of the tree branches as early as possible). The complexity of this strategy is proportional to N^K for both the CPU-time and memory. The bottleneck of this strategy is the memory needed because in order to explore the i^{th} level, the information of all the nodes of the previous level needs to be stored. It is hard to explore more than 3 levels in a complex tree search using the "breadth-first search" strategy (e.g. the tree of a target with 50,000 facets). A better way to explore the tree search of Fig. 1 is using the "depth-limited-search" method [9, 14]. As explained in detail later in this paper, this method avoids storing the information of all the nodes of the previous level. In this way, the memory needed is proportional to only KN, which means that in the practice all problems can be analyzed using an affordable amount of computer memory. The CPU-time required by the "depth-limited-search" is still proportional to N^K. Using efficient ray-tracing techniques— such as SVP, BSP, and AZB— the branches of the search-tree can be pruned early in such a way that the effective branching factor N_e of the tree search is quite less than the branching factor N of the tree. This reduction of the branching factor allows for analyses that include high order reflections.

Here we propose a new ray-tracing accelerating technique. For that the AZB algorithm is applied in a different way than in [13]. In this reference, the geometrical model was assumed to be composed of only flat facets and the reflections are treated using images: an image of the source (the primary image) for each visible facet, a secondary image for each pair of visible facets for treating double reflections, etc. This AZB application is source dependent: the images (primary and secondary) and their AZB matrices are built and stored for a particular source. This approach is efficient for treating first and second reflections, but efficiency is lost when we need to treat higher order reflections for complex models because the number of second or higher order images depends on N^K. In addition, the AZB matrices of the algorithm in [13] are source dependent. The new AZB algorithm that we propose here is not source dependent and the number of AZB matrices is limited to the number of facets in the model, N. In the new algorithm one AZB matrix is associated with each facet of the model. These matrices are not source dependent and are used in a recursive algorithm to find all the ray-paths independently of the number of reflections.

The new AZB algorithm that we propose here has some resemblance to the SBR technique, but it is fundamentally different. In SBR, rays are shot in each direction of a prefixed set of scanning directions. The rays are re-addressed after each reflection impact. No new rays are generated on any point of the ray paths. This usually implies that near the source the space is over-sampled with lots of very close rays, but far from the source or after several reflections the rays are very scarce and the space is sub-sampled. Using the SBR technique, the field at a point is computed considering some of the rays in close proximity. The AZB algorithm that we propose here defines an AZB matrix for each facet of the model and considers the possible reflections from all of the facets visible from the source. For an n-order reflection, the algorithm considers all the facets visible from the facets that have suffered the n-1 order reflection. In this way the resolution of the technique is maintained for higher order reflections. The AZB technique computes the field at a point by accurately considering all of the ray paths that left the source and suffered a specified-order reflection; there is no loss in accuracy when the reflection order increases.

The proposed ray-tracing approach has been developed in the last years to improve FASCRO, a computer code to compute the RCS based on GO-PO [6] that was not able to analyze the RCS of complex bodies considering more than two bounces with affordable computational resources. First efforts in this improvement were addressed to reduce the need of large amount of computer memory required by previous versions of the AZB algorithm. For that, the AZB was combined with the Space Volumetric Partitioning (SVP) algorithm for the analysis considering simple reflections [15] and diffraction, [16], of the RCS of electrically large and complex targets using a reduced computer memory. A very efficient approach based on the AZB and SVP algorithms combined with the A* heuristic search method, [9], was developed to consider multiple iterations between different flat surfaces, [17]. However this approach presented some fail due to the difficulty of finding a reliable way to compute the heuristic value for the RCS computations which the A* algorithm requires. In order to avoid this problem the depth-limited search strategy was proposed in [18]. A new code, called POGCROS, for an efficient computation of RCS of complex targets was implemented with all these improved algorithms and presented in [19]. In this paper we present in details the approach outlined in [18-19] together with a new version of the AZB-SVP algorithm which gives a further reduction of the CPU-time and memory resources required for analyzing large and complex problems.

This paper is organized as follows. Section II describes the AZB and SVP matrices and gives a procedure for obtaining them efficiently. The scheme proposed for speeding up the tree exploration, using a combination of AZB+SVP and the "depth-first search" algorithm is shown in Section III. This approach permits the treatment of complex targets, even for high order RCS contributions, while keeping the memory requirement affordable. The AZB+SVP scheme involves a very early pruning of the search tree, thereby reducing the search complexity. In Section IV, a detailed description of the exploration of the tree-search using the depth-limited algorithm is included. Finally, Section V presents some cases

showing the robust performance of these new ray-tracing approaches.

II. DEFINITION OF AZB AND SVP MATRICES

First, let us consider multiple reflections in a flat faceted body. We will assume a complex body modeled by many flat facets, say thousands of facets or even more. Each facet is identified by a facet number. In a pre-process we compute the AZB matrix associated with each facet. The AZB matrix of the facet with number X informs us about the visibility of the rest of facets of the model from the point of view of the X facet. To explain how this matrix is formed, let us start reviewing the AZB matrix associated with a point [6, 13].

The space viewed from a reference point can be split in angular regions that we will call anxels (an analogy with pixels). Figures 2 and 3 show an example of an anxel and space split by anxels, respectively. For simplicity, we consider angular space division for a 2D case, as shown in Fig. 4; the facets of the model are located in the 2D anxels space. Sometimes a facet extends over only one anxel, but in other cases a facet can span several anxels. The AZB technique associates a sub-matrix to each of the anxels [13]. The sub matrix of an anxel includes a list with the facet numbers of all the facets completely or partially contained in that anxel. The facet numbers in the list are ordered following the painting algorithm in an increasing order with the distance of the facet from the reference point [13]. The lists do not include the facets of the anxel that are not visible from the reference point. For example, the list for anxel 8 in Fig. 4 is: 10, 3.

As explained in [13], the AZB matrix reduces the order of complexity by searching only the facets that can reflect a ray that leaves the reference point. This search, with the help of the AZB, is performed as follows: we start by identifying the anxel corresponding with the ray direction, we check the facets whose facet numbers appear in the anxel list, and then we begin checking where the first facets on the list presumably have a high probability of being impacted by the ray.

The AZB matrix of a facet is formed combining the AZB matrices of its vertices. An anxel of the AZB of facet X contains the list of all the facets

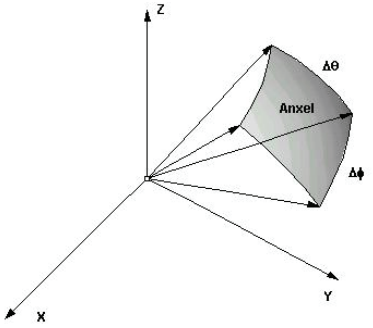

Fig. 2. Example of angular region, or "anxel" as seen from a reference point.

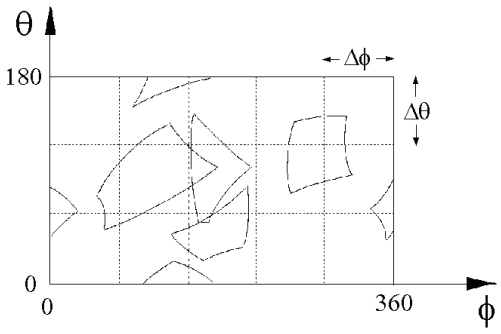

Fig. 3. The complete space seen from a point is split in anxels. The facets of the models extend over one or more anxels.

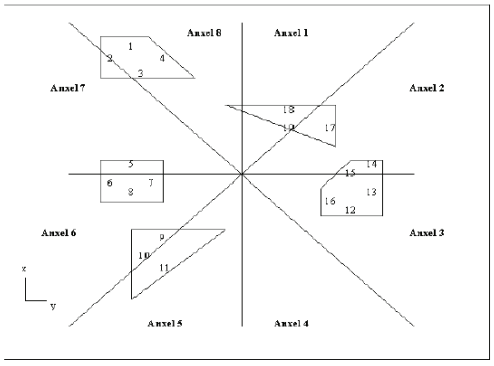

Fig. 4. Example of AZB as seen from a reference point for a 2D case.

that are seen (fully or partially) in this anxel from all the vertices of facet X. In other words, the AZB matrix of facet X is built by considering, in each anxel, the list resulting of the Boolean union of the lists in this anxel of the AZB buffers of all the vertices of facet X. The AZB of facet X contains information on how the rest of the visible facets are seen from facet X.

In addition to the AZB matrices of each facet, a particular AZB is associated with the whole structure. We call this matrix the "normal AZB matrix," which stores all the facets of the structure in accordance with the directions of the facets' normal vectors. Every facet has associated a normal vector pointing outward from the structure. The angular space of the normal AZB matrix extends over the complete angular space: 4π steroradians. In each anxel of this space we store the facets whose normal vectors are oriented into the angular range of the anxel. Only the facets that are visible from the infinite surface are considered for the normal AZB matrix.

In order to efficiently obtain the AZB matrices of the facets of a complex structure we use an adaptive version of SVP [20]. In this technique, the space containing the structure is divided into small sub-volumes called "voxels." Figure 5 shows a parallelogram containing the structure. The parallelogram is divided into smaller parallelograms or voxels. This is a first level division of the SVP. We obtain the second level division of the SVP by subdividing the small parallelograms in Fig. 5 into smaller voxels and by successively subdividing these voxels for the higher subdivision levels of the SVP. Figure 6 shows a two-level subdivision for a 2D problem, while Fig. 7 shows a three-level subdivision for the same case. In this last figure, the subdivisions are made adaptively, meaning that not all of the voxels are subdivided for a given level because if a voxel is empty or does not have small geometrical features, a subdivision is not required.

The information on the facets contained in the voxels of the lowest level of subdivision together with the relation between the voxels in an adaptive SVP subdivision is stored in a relational database of matrices. We use Fig. 7 to explain how we can take advantage of the SVP method. For instance, if we want to know if there is any facet obstructing the segment which joins the centers of facets 16 and 31 in Fig. 7, we only need to check for a possible obstruction to the facets contained in voxels: (1)-(a)/(1)-(a); (1)-(b)/(1)-(a); (1)-(b)/(1)-(b); (2)-(a)-(i)/(1)-(b)-(j); and (2)-(2). To obtain the AZB matrix of facet 31, we shall explore for each of the vertices of facet 31 in which angular region are the rest of facets of Fig. 7—if they are visible from these vertices.

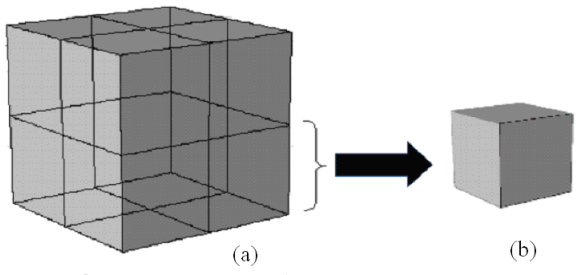

Fig. 5. Example of a first level division of a volume into 8 sub-volumes or voxels.

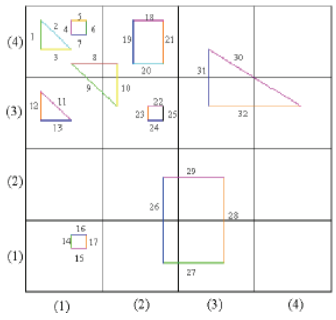

Fig. 6. Example of a two level, uniform SVP for a 2D case.

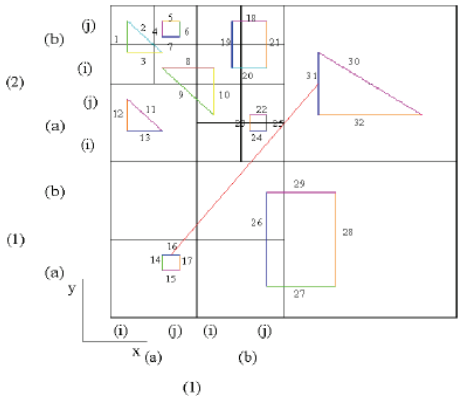

Fig. 7. Application of the adaptive SVP to find the facets in the line joining the centers of facets 16 and 31. Three non uniform levels are considered.

III. APPLICATION OF THE RECURSIVE AZB+SVP ALGORITHMS FOR RCS COMPUTATIONS

AZB+SVP can be applied recursively to compute the RCS of a complex structure composed of flat facets. We assume that the total number of facets N is very large. This approach is applicable to monostatic or bistatic RCS computations. The directions of incidence and

observation are defined by the unit vectors $\hat{k}_i$ and $\hat{k}_o$, respectively (where $\hat{k}_i = \hat{k}_o$ for monostatic RCS)

A. Computation of the RCS Due to Simple Reflections

The contribution to the RCS from each illuminated facet for simple reflection is computed using Gordon´s expressions for the evaluation of the PO integral that gives the far field radiated by currents of constant amplitude and phase with a lineal variation [4]. A very rough way to select the facets that can potentially be illuminated is by applying the Culling's criterion for the incidence and observation directions (the facets of the structure that are simultaneously seen in the incidence and observation directions) [13]. A facet with normal unit vector $\hat{n}$ is classified as potentially illuminated applying this criterion if the following expressions of scalar vector products are simultaneously satisfied:

$$\hat{n} \circ \hat{k}_i \leq 0 \qquad (1)$$

$$\hat{n} \circ \hat{k}_o \geq 0. \qquad (2)$$

The application of the Culling's criterion reduces the complexity of the problem from order N to order N/2. However, we can furthermore reduce the complexity of the problem by taking into account that the contribution to the bistatic RCS of a flat facet vanishes when the directions of incidence and observation are far away, following Snell's law for the reflection off this facet (see Fig. 8):

$$\left|\hat{n} \circ \hat{k}_i\right| = \left|\hat{n} \circ \hat{k}_o\right|. \qquad (3)$$

We shall consider facets that are finite in size; the PO solution gives a scattered field in a narrow beam of width $\Delta\Phi$ around the Snell direction of reflection. Therefore, given the directions of incidence and observation, we shall consider facets as potential RCS contributors only if their normal vectors follow this relation:

$$\hat{n} \circ \left(\frac{\hat{k}_i + \hat{k}_o}{\left|\hat{k}_i + \hat{k}_o\right|} \right) \geq cos(\ \Delta\Phi\ ). \qquad (4)$$

We can select all the facets that follow (4) very efficiently by considering all of the facets in the anxel of the "*normal AZB matrix*" that include into their angular window the direction:

$$\hat{n}_s = \frac{\hat{k}_i + \hat{k}_o}{\left|\hat{k}_i + \hat{k}_o\right|}. \qquad (5)$$

When only the facets in the anxel of $\hat{n}_s$ are taken as potential contributors, the complexity of the problem is reduced to $N/(N_\theta N_\varphi)$, where N_θ and N_φ are the divisions on the entire angular space considered in the "*normal AZB matrix*" for the θ and φ spherical coordinates, respectively. Typically, the factor $N_\theta N_\varphi$ is about 400 and, therefore, using the "*normal AZB matrix*" reduces much of the complexity for problems involving simple reflections. In the case where $\hat{n}_s$ is close to the boundaries of its anxel in the "*normal AZB matrix*," or when the angular range of this anxel is less than the width $\Delta\Phi$ of the PO reflected beam, we select the facets located in this anxel and on its neighboring anxels (typically the 8 surrounding anxels); we notice that the complexity of this problem is also largely reduced.

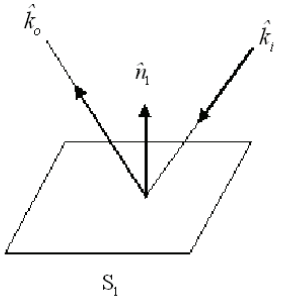

Fig. 8. Visualization the a case where the incidence direction vector $\hat{k}_i$, observation direction vector $\hat{k}_o$ and normal vector $\hat{n}_1$ follow or are close to Snell's law at surface S_1.

Once we have selected the set of facets that potentially contribute to the RCS using the fast procedure described above, we will determine if each facet contributes to the RCS and if we should trim its surface before applying Gordon's law to take into account partial occultation to correctly compute the PO integral. Some of the facets of this set cannot contribute to the RCS because they are shadowed by other facets that can occlude the

incident ray or the reflected ray in the observation direction. To determine which facets shadow the incident ray that illuminates facet *f*, we only consider the facets in the anxel that contains the incident direction $\hat{k}_i$ of the AZB of facet *f*. We apply rigorous algorithms to these facets [13]; the algorithms allow us to discover if facet *f* is completely or partially occluded by other facets when it is illuminated in the incident direction $\hat{k}_i$. In the case that facet *f* is partially occluded, its surface S_f shall be trimmed, saving for PO evaluation only the illuminated surface area S_f^i. Figure 9 shows an example of a facet trimming.

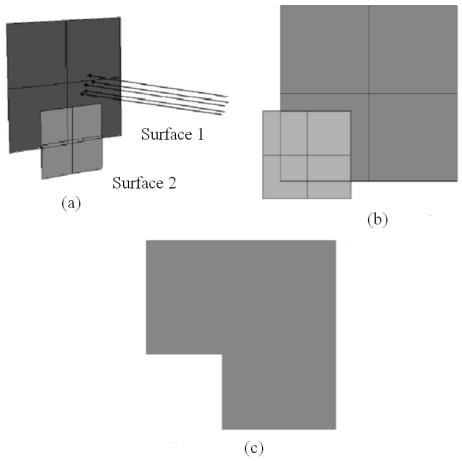

Fig. 9. An example of trimming the surface of a facet when it is partially occluded by another facet that intersects the incident rays.

After reflection on facet *f* we can assume that the reflected fields are located in a cylindrical tube of collimated rays parallel to the direction of reflection. This tube can suffer a total or partial occlusion from some of the facets of the structure. In the case of a total occlusion, we can state that facet *f* is shadowed in the observation direction $\hat{k}_o$ and therefore does not contribute to the RCS. In the case of partial occlusion, we will compute the trimming of the reflected tube section; after trimming the tube will have a surface S_f^{io}. We only employ rigorous algorithms for facet occlusion computations to the facets in the anxel of the AZB of facet *f* that contains the observation direction $\hat{k}_o$ in order to only select the facets that can potentially occlude the tube of rays reflected by facet *f*, as shown in Fig. 10 [13].

We note that applying the rigorous algorithms for determining if a facet is shadowed completely or partially in either the incidence or observation directions by other facets, and in this case the corresponding trimming, is time consuming and shall be applied only to the facets that have a chance to occlude facet *f*. The AZB of facet *f* permits us to select the facets that can potentially occlude facet *f*, lowering the complexity of the problem by a factor of $N/(N_1N_2)$, where N_1N_2 is the number of anxels considered in the AZB of the facets.

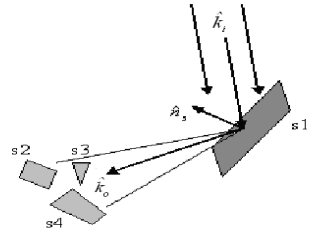

Fig. 10. Only the facets included in the anxel AZB of facet S1 that contain the direction $\hat{k}_o$ are considered for studying of the occultation of the tube of rays reflected in S1.

B. Computation of the RCS Due to Double Reflections

The contribution to the RCS by double reflection between pairs of facets is computed using GO+PO. GO is applied to study the reflection on the first facet, while Gordon's expression is used to evaluate the PO integral of the current induced in the second facet. The ray-tracing approach starts by selecting the facets that can suffer the first reflection, following the procedure described above: facets not visible in the incident direction are discarded using the Culling's criterion; the surfaces that shadow a potentially illuminated facet are those located in the anxel of the AZB of the facet that contains the direction of incidence $\hat{k}_i$; rigorous checking algorithms for shadowing are applied only to the facets located in this anxel and the surface of the illuminated facets partially occluded is trimmed.

A reflected cylindrical tube of rays is formed for each facet that suffer the first reflection. The tube of rays follows the direction given by the Snell's law after the reflection in the illuminated facets. The tubes can bounce on some of the facets of the structure, and these secondary facets give the double reflection. These facets are located in

the anxels that contain the direction of reflection of the AZB of the facets from which the tube of rays emanates. The rigorous checking algorithms for shadowing are only applied to the facets of these anxels. The facets of these anxels that are partially illuminated by the tube of rays are trimmed.

The last step in the computation of double reflection is applied only to the set of facets completely or partially illuminated by the tubes of rays formed after the first reflection. When the tubes from this set suffer a second reflection, they change their direction of propagation following Snell's law. We note that due to its finite section, the tube of rays redirected by a facet becomes a narrow beam of width $\Delta\Phi$ around the direction of reflection in the far field. Therefore, if the direction of observation $\hat{k}_o$ is outside this beam, this facet does not contribute to the RCS in that direction of observation. Elsewhere, the facet can potentially contribute to the RCS due to double reflection. We shall check if the redirected tube is partially or totally occluded by the other facets of the structure. To efficiently treat this new occlusion study, we apply the rigorous checking algorithms only to the facets located in the anxel that contains the $\hat{k}_o$ direction of the AZB of the facet that suffers the second reflection. If the tube is partially occluded, we shall trim again the section of the tube in the surface of the facet that suffers the second reflection. The computation of the PO integral is performed only over the surfaces of the facets whose redirected tubes of rays have not been completely occluded.

We notice that when using only the Culing's criterion without the AZB algorithm, the complexity of the problem for a given incidence and reflection directions is proportional to $N^2/4$ for finding the pairs of facets that can contribute to the double reflection and the complexity is proportional to $3N^3/4$ for finding the potential occlusions by other facets in each one of the three segments of a ray path that underwent double reflection (from the source to the first facet of the pair, between the facets of the pair and from the second facet of the couple and the observation point). Using the AZB algorithm and the Culling's criterion the complexity is reduced to $N^2/(2(N_1N_2))$ for finding the pair of facets that can give a double reflection, and the complexity is reduced to $3N^3/(2(N_1N)^2)$ for finding the facets that can potentially occlude any one of the three segments of a double reflection ray-path.

C. Computation of the RCS Due to Triple and Higher Order Reflections

The contribution to RCS due to m-order reflections is related to sets of m-facets. In each set the field incident in the $\hat{k}_i$ direction is reflected by the first facet and its direction of propagation is redirected following Snell's law. The reflected field suffers consecutive reflections until it reaches the last facet of the set where the field is radiated in a beam that contains the direction of observation $\hat{k}_o$. The tube of rays that bounces the first facet will likely suffer successive trimming due to partial occlusions during its propagation along the ray path connecting the facets of the set. Finding the sets of m-facets that give m-order reflections and computing trimming for the tubes of rays after successive occlusions is undoubtedly a hard and cumbersome process. Without using a ray-tracing algorithm (except for Culing's criterion), the complexity of the problem for finding the contributing sets of m-facets is proportional to $(N/2)^m$ and the complexity of finding the occlusion of the tubes of rays proportional to $(m+1)\ (N/2)^{m+1}$. Using the AZB algorithm, the complexity of the problem is reduced to $(N^m/2)/(N_1N_2)^{m-1}$ for finding the groups of m-facets and to $(m+1)(N^{m+1}/2)(N_1N)^m)$ for finding the occlusions in the (m+1) segments of the ray paths.

Applying AZB for the first and last reflections is similar to the case of double reflection. The treatment of the reflection i^{th} is as follows:

- First, we study the facets potentially illuminated by the tube of rays reflected by the facet *i-1*. To do so, we consider all the facets in the anxel of the AZB of facet *i-1* that contains the direction of propagation of the tube. We apply rigorous algorithms to the facets of this anxel to accurately check if the illumination is total or partial. The tube of rays is trimmed after the occlusion in every facet that suffers total or partial occultation in the trajectory from the $(i\text{-}1)^{th}$ reflection to the i^{th} reflection.

- A new tube of rays is formed in every facet that undergoes the i^{th} reflection. The directions of these tubes are given by Snell´s law and their

section is formed by trimming the surfaces of every one of these facets with the incident tubes of rays in order to maintain only the illuminated parts. This trimming is performed using rigorous algorithms. Using these tubes of rays we can proceed to study the $(i+1)^{th}$ reflection.

IV. COMBINING AZB+SVP WITH THE DEPTH-LIMITED-SEARCH METHOD

A procedure for implementing the depth-limited-search method for exploring the search tree in Fig. 1 is summarized in the following paragraphs. The scheme permits the computation the RCS of a complex-faceted geometry. The maximum order or reflection is limited to N_{order}, the number of levels to be considered in the search tree.

Figure 11 is a flow chart of the new algorithm based on the combination of SVP+AZB with the depth-limited-search method.

1. The nodes of the first level in the search tree of Fig. 1 correspond to those facets that can be the first in the pair of facets that gives an n-order contribution to the RCS for prefixed incident and observation directions and any value of n. The facets of the first level are selected among all of the facets of the geometry considering back-face culling: the facets of the structure that are seen in the incidence direction (see appendix 3.b of [13]). These facets are considered as "active" surfaces and are stored in a list called OPENLIST. The facets are sorted in this list in an increasing order following the facet index, which is a number in the geometry database used for identifying the facets. Account number I_{level} is made equal to one and it is associated with each of the facets stored in OPENLIST.

2. The surface with the smallest facet order in OPENLIST, which is the first facet in that list, is selected. This surface is moved to the file ACTUAL and then removed from OPENLIST. The contribution to the RCS for the first reflection in the observation direction is computed using the algorithms described above in Section III.

3. If the I_{level} count of facets in ACTUAL is less than N_{order}, then next step is to update OPENLIST by inserting a new set of active surfaces into the list, or else the procedure skips to step 4. They are selected from the anxel of the AZB matrix of the surface in ACTUAL that contains the Snell reflection direction of that facet. The surfaces in

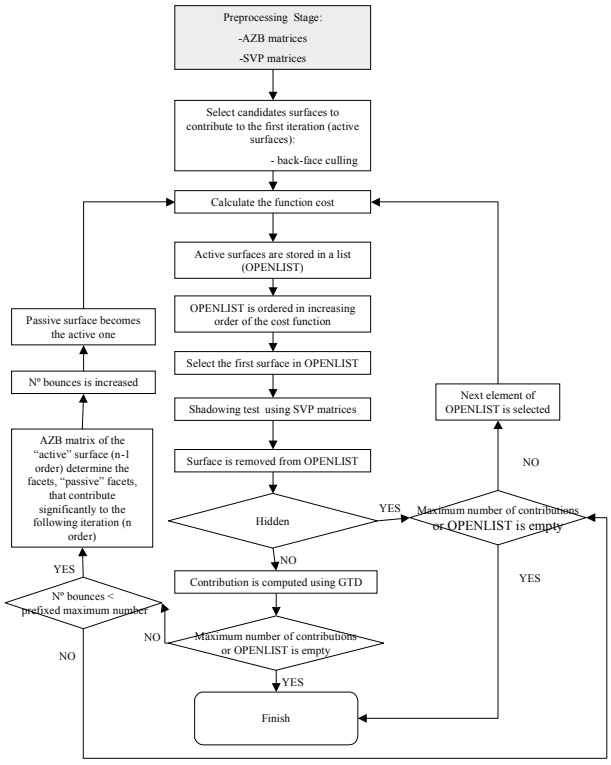

Fig. 11. Flow chart of AZB+SVP combined with the depth-limited-search method.

that anxel are inserted into the first spots in OPENLIST in increasing order of their facet index. The account number I_{level} associated with the new facets inserted in OPENLIST is the account number of ACTUAL plus one. We note that the new facets inserted in OPENLIST are placed in front of all of the facets previously stored in OPENLIST, and therefore the list can be classified as LIFO (last input-first input). The facet is then removed from ACTUAL.

4. The first facet in OPENLIST is removed and inserted in ACTUAL; the RCS contribution of this facet is computed following the procedure indicated in part 3 for a second or higher order reflection. Steps 3 and 4 are repeated.

The process is completed when all of the elements have been analyzed (OPENLIST is empty).

V. RESULTS

To show the performance of the new algorithm, several results are presented with an increasing difficulty. In all the cases presented the targets are

perfect electric conductors. The first case is the set defined by the dihedral and trihedral pictured in Fig. 12. The sides of both entities (dihedral and trihedral) are formed by flat 1.0m x 1.0m squares. The trihedral has its vertex at the origin of a Cartesian coordinate system with its sides parallel to the coordinate planes. The dihedral has one side parallel to the z=0 plane and the other parallel to the x = -y plane, as shown in Fig. 12. The coordinates of the mid-point of the edge of the dihedral are (2, 2, 1). The geometry of the case has been designed to show scattering with a large and rich number of interactions between the sides of the two entities of the figure when the set is illuminated by incident waves in the plane ϕ=45° (of the associated cylindrical coordinates). The structure undergoes multiple reflections/ diffractions. Until fifth order reflections are generated. Figures 13-14 show a comparison between RCS values for the geometrical approach using MONURBS [21], a moment method (MM) code, and POGCROS a computer code implemented using the present approach. In order to obtain reliable results, POGCROS was run computing until sixth order reflections. The results were stable if the effects order was increased until ten—in other words, for the incidence direction considered, sixth or higher order reflections are negligible. From the comparison between the MM results and the present approach we notice good agreement, considering the limitations of a GO-PO approach and the rich of mutual iterations of the test case in Fig. 12. The CPU-times using POGCROS (run in a Pentium Dual Core (2.5 GHz) using only one processor) have been of 50 s and 52 s for the cases with a maximum of 6 and 10 bounces, respectively.

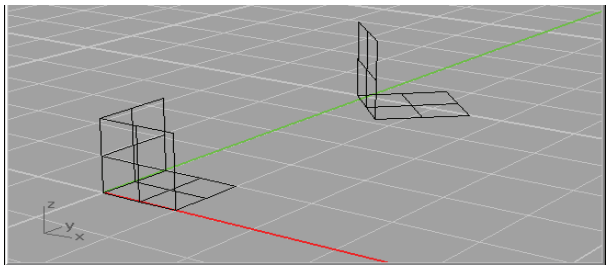

Fig. 12. Geometrical set defined by a dihedral and a trihedral designed in order to maximize the number of multiple reflections between the sides of the set.

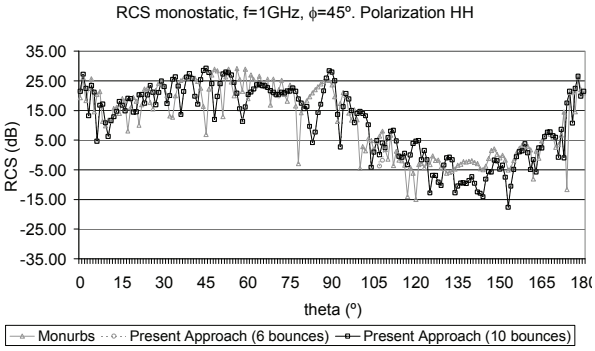

(a)

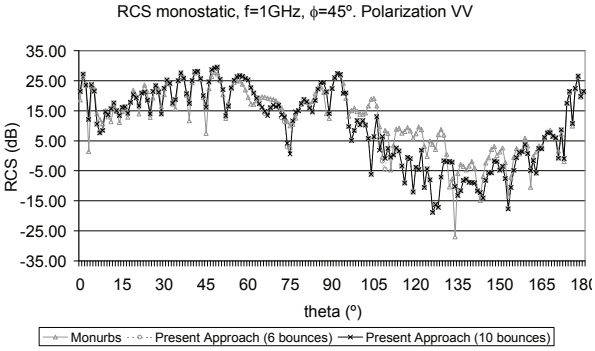

(b)

Fig. 13. Comparison between the values of the monostatic RCS for the geometrical structure in Fig. 12 obtained using MONURBS and the present approach for Φ =45°, for HH (a) and VV (b) polarizations and a frequency of 1 GHz.

Previous cases are suitable for analyzing the reliability of our proposed approach for simple problems with multiple reflections. We present here two examples to show the improvement in computational efficiency in terms of memory and CPU-time of our approach when complex problems are analyzed. The first case, called Placyl, is a hemisphere-cylinder above a flat plate as shown in Fig. 15. The radius of the hemisphere and of the cylinder is 0.2 m, the length of the cylinder is 1 m and the dimensions of the plate are 1.8 m and 1.2 m. The axis of the cylinder is parallel to the longer side of the plate and there is a gap between the cylinder and the plate of height 0.02 m. The Placyl case has been modeled by 1038 flat surfaces. Figure 16 shows the monostatic results obtained for HH and VV polarizations for a θ =45º cut and a sweeping from Φ =0º to Φ =180º

running POGCROS with a maximum of six bounces.

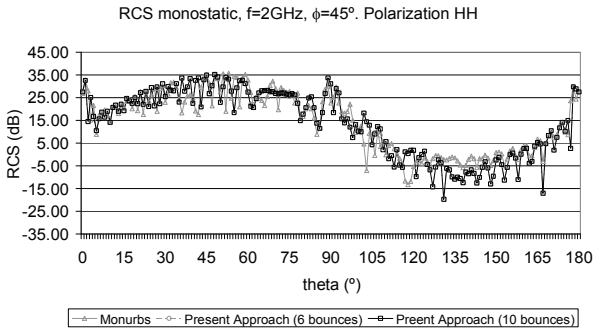

(a)

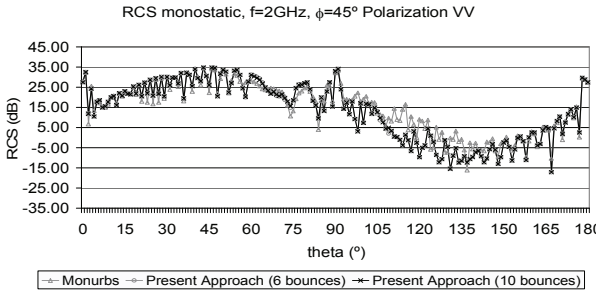

(b)

Fig. 14. Comparison between the values of the monostatic RCS for the geometrical structure in Fig. 12 obtained using MONURBS and the present approach for Φ =45°, HH (a) and VV (b) polarizations and a frequency of 2 GHz.

The comparison between the results obtained with MONURBS and POGCROS show a reasonably good agreement between MM and GO+GO...+PO approaches. The results of POGCROS have been run in a Pentium Dual Core, 2.5 GHz, using only 56 MB of RAM and a CPU-time of 5 min 21 sec.

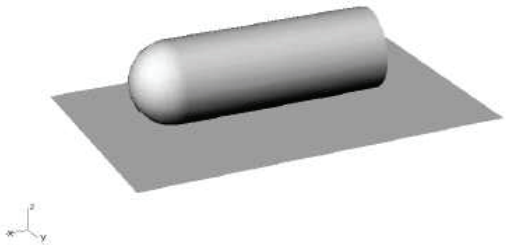

Fig. 15. Geometric model and coordinates system of the "placyl" case.

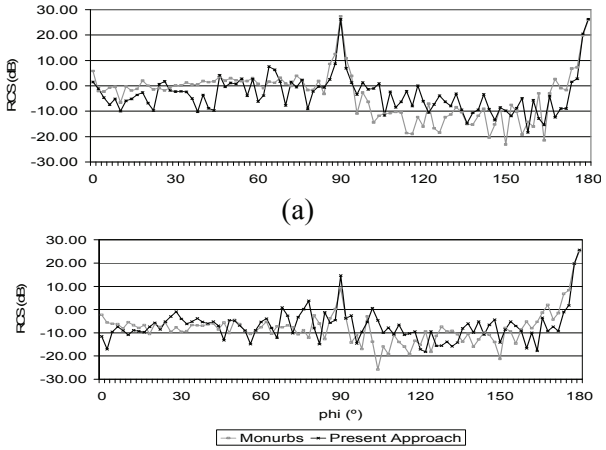

(a) (b)

Fig. 16. Comparison between the values of the monostatic RCS for the plane-cylinder geometrical structure shown in Fig. 15 obtained using MONURBS and the present approach for Φ =45°, HH (a) and VV (b) polarizations and a frequency of 10 GHz.

Fig. 17 . Flat faceted model of T72 tank.

The last and more complex example presented here is a geometrical model of a T72 tank composed of 22,225 flat facets, as shown in Fig. 17. First, we study the reliability of the results obtained using present approach (POGCROS) for this complex target. To do so, in Fig. 18 we compare RCS results for the T72 tank obtained using POGCROS and FASCRO. This last code is a well tested computer tool that can be considered as a previous version of POGCROS. The FASCRO code is based on an electromagnetic approach kernel similar to that used by POCROS to compute the RCS [6], but with a less efficient ray-tracing engine that is not able to treat more than two bounces with affordable computational resources. Due to this limitation of FASCRO, the comparison in Fig. 18 considers a maximum of two bounces. We note that the results obtained with both codes agree very well. However, the

computational resources required for obtaining the RCS values for the 360 directions in Fig. 18 are very different, as can be seen in table 1 where the superior efficiency of POGCROS is quite clear (a SUN V40Z computer has been used for all the T72 calculations in this paper).

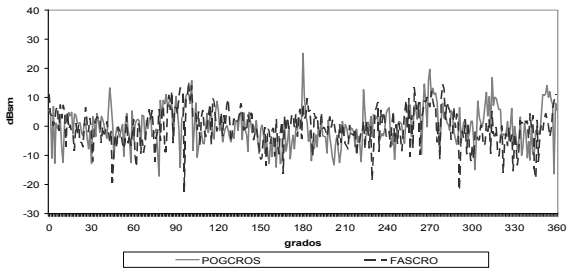

Fig. 18. Comparison between monostatic RCS results obtained using FASCRO and POGCROS for the cut θ = 72º, from Φ = 0º to Φ = 360º at 10 GHz and vertical polarization.

The POGCROS code has been used to study the impact on the RCS values from the maximum number of bounces in the ray-tracing. The RCS of a large and complex target, as it is the case for the T72, fluctuates very fast when we consider a step of a degree in a given cut, as for example the θ=72º cut. Due to these fast fluctuations it is difficult to obtain conclusions from RCS diagrams obtained when considering different values for the maximum number of bounces when they are drawn together. To avoid these problems, we consider windowed values of the RCS for each direction in the cut. Figure 19 show the averaged RCS values for each direction considering a 5 degree width flat window (the value shown for a given direction Φ_a is the average of the RCS in dBm considering the five directions contained in angular sector of 5 degrees centered at Φ_a). Figure 19 show results obtained considering 2, 3 and 6 bounces. The convergence is obtained considering 6 or more bounces. It can be noticed that the results obtained considering a maximum of only 2 bounces are not accurate enough compared with the results with a maximum of 6 bounces. Therefore, for the complex T72 target, it is evident that one needs to have available computer tools that are able to analyze the RCS considering 3 or more bounces with affordable computational resources. Table 2 shows the CPU-time and computer memory required for obtaining the RCS of the T72 for the 360 possible directions and a given maximum number of bounces. A SUN V40Z computer was used for all of the simulations

Table 1: Comparison between the CPU-time and computer memory required by FASCRO and POGCROS for obtaining the results of Fig. 21.

Code	CPU-time	Memory
POGCROS	1h, 45m, 33s	200 MB
FASCROS	8h, 52m, 32s	2 GB

Table 2: CPU-time and memory required by both polarizations considering several values of the maximum number of bounces in the RCS analysis.

Maximum number of bounces	Polarization vv	Polarization hh	Memory
2	1h, 45m, 33s	1h, 44m, 40s	200 MB
4	1h, 56m, 22s	1h, 54m, 23s	200 MB
6	2h, 00m, 15s	1h, 59m, 29s	200 MB
10	2h, 02m, 40s	2h, 01m, 56s	200 MB

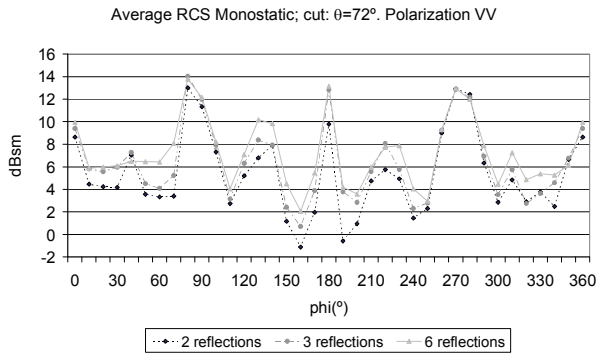

(a)

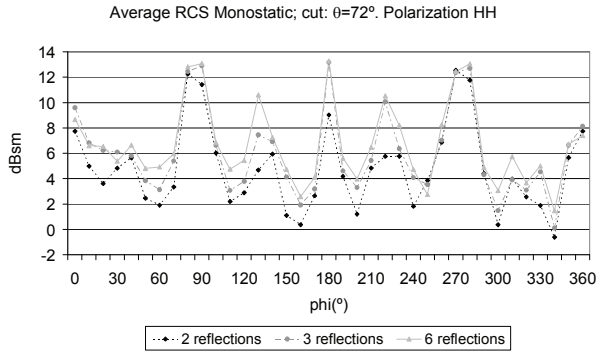

(b)

Fig. 19. Convergence study of the averaged monostatic RCS at 10GHz for VV and HH polarizations changing the maximum number of bounces considered.

in table 2. We note that the increase in computer resources to consider 3 or more bounces is negligible.

VI. CONCLUSIONS

An approach that combines an electromagnetic model based on GO and PO and a new ray-tracing scheme for the analysis of the Radar Cross Section (RCS) of complex structures that considers any number of bounces is presented. The structures are modeled by flat surfaces. The new ray-tracing scheme presented is based on a combination of the angular Z-buffer (AZB), volumetric space partitioning (SVP) and depth-limited-search methods and it is very efficient for computing the RCS of large and complex bodies. Several results have been presented for simple targets to show the accuracy of the approach. When analyzing large and complex targets, where one needs to take into account 3 or more bounces, we prove that the approach needs a very small amount of computer memory and affordable CPU-times.

Currently the authors are extending this approach to find the RCS of bodies modeled by curves surfaces. The approach has recently been implemented for analysis of radiating sources near complex bodies [22]. In a preprocessing stage of the approach, the curved surfaces are converted into small facets according to the curvature of the surface. Thus, the reflection points are calculated on the facets by applying image theory and the Z-buffer algorithm. This ray-tracing algorithm is able of computing n-order bounces. Once the *n* points of reflection are calculated they are used as a point seed in a conjugate gradient algorithm that is used to accurately compute the real reflection points on the curved surface.

ACKNOWLEDGMENTS

This work has been supported, in part by the Comunidad de Madrid and S-0505/TIC/0255 and by the Spanish Department of Science, and Technology Projects TEC 2007-66164 and CONSOLIDER-INGENIO Nº CSD-2008-0068.

REFERENCES

[1] N. N. Youssef, "Radar Cross Section of Complex Targets", *Proceedings of the IEEE,* vol. 77, no. 5, May 1989, pp. 722-734.

[2] E. F. Knott, "A Progression of High Frequency RCS Prediction Techniques", *Proceedings of the IEEE,* vol. 73, no. 2, pp. 252-264, February 1985.

[3] A. Michaeli, "Equivalent edge currents for arbitrary aspects of observation", *IEEE Transactions on Antennas and Propagaion.,* vol. AP-32, pp. 252-258, Mar. 1984.

[4] W. B. Gordon, "Far-Field Approximation to the Kirchoff-Helmhotz Representations of Scattered Field", *IEEE Transactions on Antennas and Propagation,* vol. AP-23, pp. 864-876, July 1975.

[5] D. S. Jones and M. Kline, "Asymptotic expansions of multiple integrals and the method of the stationary phase", *J. Math. Phys.,* vol. 37, pp. 1-28, 1957.

[6] F. Saez de Adana, I. González, O. Gutiérrez, P. Lozano, and M.F. Cátedra, "Method Based on Physical Optics for the Computation Radar Cross Section Including Diffraction and Double Effects of Metallic and Absorbing Bodies Modeled With Parameter surfaces", *IEEE Trans. on Antennas and Propagation,* vol. AP-53, pp. 3295-3303, Dec. 2005.

[7] T. Griesser and C. A Balanis, "Backscatter Analysis of Dihedral Corner Reflectors Using Physical Optics and Physical Theory of Diffraction", *IEEE Transactions on Antennas and Propagation,* vol. AP-35, pp. 1137-1147, Oct. 1989.

[8] J. Baldauf, S. W. Lee, L. Lin, S. K. Jeng, S. M. Scarborough, and C. L. Yu, "High Frequency Scattering From Trihedral Corner Reflectors and Other Benchmark Targets: SBR Versus Experiment", *IEEE Transactions on Antennas and Propagation,* vol. AP-39, pp. 1345-1351, Sept. 1991.

[9] S. Russel and P. Norvig, *Artificial Intelligence: a Modern Approach,* Prentice Hall, 2003.

[10] H. Ling, R. Chou, and S. W. Lee, "Shooting and Bouncing Rays: Calculating the RCS of an Arbitrarily Shaped Cavity," *IEEE Transactions on Antennas and Propagation,* vol. AP-37, pp. 194-205, Feb. 1989.

[11] D. J. Andersh, M. Hazlett, S. W. Lee, D. D. Reeves, D. P. Sullivan and *Y.* Chu, "Xpatch: A High Frequency Electromagnetic Scattering Prediction Code and environment for Complex Three-Dimensional Objects," *IEEE Antennas and Propagation Magazine,* vol. 36, pp. 65-69, Feb. 1994.

[12] J. Perez, F. Saez de Adana, O. Gutierrez, I. Gonzalez, M. F Cátedra, I. Montiel, and J. Guzman, "FASANT: Fast Computer Tool for the Analysis of on board Antennas", *IEEE Magazine on Antennas & Propagation,* pp. 15-28, Apr. 1999.

[13] M. F. Cátedra and J. Pérez-Arriaga, *Cell Planning for Wireless Communications,* Artech House Publishers, 1999.

[14] G. F. Luger, *Artificial Intelligenc. Sructures and Strategies for Complex Solving,* Addisson Wesley, 2005.

[15] L. Lozano, M. I. Hernández, C. Romera, I. González, F. Saez de Adana, and M. F. Cátedra, "Ray-Tracing acceleration techniques to compute RCS of complex targets", *IEEE Antennas and Propagation Society Symposium,* pp. 4495-4498, June 2004.

[16] L. Lozano, E. Ortega, F.Saez de Adana, and F, Catedra, "Improvements in ray-tracing acceleration techniques to compute diffraction effect and doubles and triples effects in the RCS prediction of complex targets", *IEEE Antennas and Propagation Society International Symposium,* vol. 3A, pp. 93- 96, July 2005.

[17] L. Lozano, I. Gonzalez, O. Gutierrez, J.M. Gomez, and F. Catedra, "Iterative method for computing N - reflections between flat surfaces in the RCS prediction of complex targets", *IEEE Antennas and Propagation Society International Symposium,* pp. 2502-2505, June 2007.

[18] L. Lozano, M.J. Algar, M. Blanco, I. Gonzalez, and F. Catedra, "Depth limited search applied to compute N-order reflections in the analysis of the RCS in large and complex targets", *IEEE Antennas and Propagation Society International Symposium,* vol. AP-S, pp. 1-4, July 2008.

[19] M. J. Algar, L. Lozano, I. Gonzalez, F. Catedra, "An efficient approach to compute the RCS of complex targets consideringmultiple bounces", *Antennas and Propagation, (EuCAP),* pp. 3703-3707, March 2009.

[20] V. Havran, *Heuristic Ray Shooting Algorithms*, Dissertation Thesis, November 2000.

[21] I. González, E. Garcia, F. Saez de Adana, and M. F. Cátedra, "MONURBS: A Parallelized Multipole Multilevel Code for Analyzing Complex Bodies Modeled by NURBS Surfaces", *Applied Computational Electromagnetics Society Journal,* vol. 23, no. 2, pp. 134-14, June 2008.

[22] F. Cátedra, L. Lozano, and I. Gonzalez, "New Algorithm for Computing Antenna Iterations with flat/curved Structures considering any Number of Bounces**"**, *30th ESA Antenna Workshop on Antennas,* pp. 551-554, May 2008.

Manuel F. Catedra received his M.S. and Ph. D. degrees in Telecommunications Engineering from the Polytechnic University of Madrid (UPM) in 1977 and 1982 respectively. From 1976 to 1989 he was with the Radiocommunication and Signal Processing Department of the UPM. He has been Professor at the University of Cantabria from 1989 to 1998. He is currently Professor at the University of Alcalá, in Madrid, Spain. He is a Fellow of the IEEE.

He has worked on about 90 research projects solving problems of Electromagnetic Compatibility in Radio and Telecommunication Equipment, Antennas, Microwave Components and Radar Cross Section and Mobile Communications. He has developed and applied CAD tools for radio-equipment systems such as Navy-ships, aircraft, helicopters, satellites, the main contractors being Spanish or European Institutions such as EADS, ALCATEL, CNES, ALENIA, ESA, DASA, SAAB, INTA, BAZAN, INDRA, the Spanish Defence Department.

He has directed about 15 Ph D. dissertations, has published about 60 papers (IEEE, Electronic Letters, etc), and two books.

Lorena Lozano Plata was born in Madrid, Spain in 1978. She received the BS, MS and PhD. Degrees in Telecommunications Engineering from the University of Alcalá, Spain, in 2000, 2002 and 2006, respectively. Since 2005 she works at the University of Alcalá, fist as Faculty Research

and since 2007 as Professor. She has worked as Faculty Research at Arizona State University from May 2004 to November 2004.
Her areas of interest are on-board antennas analysis, radio propagation on mobile communications, ray-tracing techniques and high frequency techniques, where she has worked on about forty research projects solving problems of Radar Cross Section computation, analysis of on board antennas, Mobile Communications, radio propagation, etc.
She has given short courses and has given about twenty presentations in International Symposium. She has authored four papers in referred journals and in chapters in a book.

Iván González Diego was born in Torrelavega, Spain in 1971. He received the B.S. and M.S. degrees in telecommunications engineering from the University of Cantabria, Spain, in 1994 and 1997 respectively, and the Ph.D degree in telecommunications engineering from the Univeristy of Alcalá , Madrid, Spain in 2004.

He worked in the Detectability Laboratory of the National Institute of Technical Aerospace (INTA), Madrid, Spain in RCS prediction and measurements and as Assistant Researcher at the University of Alcalá. Since 2004, he works as Assistant Professor in the University of Alcalá in the Computation Science Department teaching concepts about Data Base Systems. He has participated in several research projects with Spanish and European companies, related with analysis of on board antennas, radio propagation in mobile communications, RCS computation, etc. His research interests are in numerical methods applied to the electromagnetic problems, rigorous and asymptotic techniques like Method of Moments, GTD/UTD, PO, etc. He is also interested in the numerical methods to represent complex bodies for the electromagnetic techniques and compuer graphics is one of his research area.

Eliseo Garcia was born in Madrid, Spain, in 1977. He received the B.S., M.S. and Ph.D. degrees in telecommunication engineering from the University of Alcalá, Spain, in 1999, 2001 and 2005, respectively.
Since 2005, he worked at the University of Alcalá, first as Assistant Professor and since 2006 as Associated Professor in the Automatic Department. His research interests include numerical methods applied to scattering and radiation problems, parallel computing and fast computational techniques applied to electromagnetics.

María Jesus Algar Díaz was born in Madrid, Spain in 1984. She received a MS (2007) in Telecommunications Engineering from Alfonso X El Sabio University, Spain. She is currently pursuing a PhD. in Tlecommunications from University of Alcalá, where she works as Research. Her current research interests include analysis of on-board antennas, radio propagation on mobile communications, ray-tracing techniques and high frequency techniques.